Research Article | Vol. 26, No. 9 | 30 Apr 2018 | OPTICS EXPRESS 11889

Optics EXPRESS

Suppressing the photobleaching and photoluminescence intermittency of single near-infrared CdSeTe/ZnS quantum dots with *p*-phenylenediamine

CHANGGANG YANG,[1,2] GUOFENG ZHANG,[1,2,4] LIHENG FENG,[3] BIN LI,[1,2] ZHIJIE LI,[1,2] RUIYUN CHEN,[1,2] CHENGBING QIN,[1,2] YAN GAO,[1,2] LIANTUAN XIAO,[1,2,5] AND SUOTANG JIA[1,2]

[1]*State Key Laboratory of Quantum Optics and Quantum Optics Devices, Institute of Laser Spectroscopy, Shanxi University, Taiyuan, 030006, China*
[2]*Collaborative Innovation Center of Extreme Optics, Shanxi University, Taiyuan, Shanxi, 030006, China*
[3]*School of Chemistry and Chemical Engineering, Shanxi University, Taiyuan, 030006, China*
[4]*guofeng.zhang@sxu.edu.cn*
[5]*xlt@sxu.edu.cn*

Abstract: Intrinsic photobleaching and photoluminescence (PL) intermittency of single quantum dots (QDs), originating from photo-oxidation and photo-ionization respectively, are roadblocks for most single-dot applications. Here, we effectively suppress the photobleaching and the PL intermittency of single near-infrared emitting QDs with *p*-phenylenediamine (PPD). The PPD cannot only be used as a high-efficient reducing agent to remove reactive oxygen species around QDs to suppress the photo-oxidation, but can also bond with the surface defect sites of single QDs to reduce electron trap states to suppress the photo-ionization. It is shown that the survival time of single QDs, the on-state probability of PL intensity traces, and the total number of emitted photons are significantly increased for single QDs in PPD compared with that on glass coverslip.

OCIS codes: (300.6500) Spectroscopy, time-resolved; (300.2530) Fluorescence, laser-induced; (160.4236) Nanomaterials.

References and links

1. M. R. Kim and D. Ma, "Quantum-dot-based solar cells: recent advances, strategies, and challenges," J. Phys. Chem. Lett. **6**(1), 85–99 (2015).
2. Q. Huang, J. Pan, Y. Zhang, J. Chen, Z. Tao, C. He, K. Zhou, Y. Tu, and W. Lei, "High-performance quantum dot light-emitting diodes with hybrid hole transport layer via doping engineering," Opt. Express **24**(23), 25955–25963 (2016).
3. J. M. Pietryga, Y. S. Park, J. Lim, A. F. Fidler, W. K. Bae, S. Brovelli, and V. I. Klimov, "Spectroscopic and device aspects of nanocrystal quantum dots," Chem. Rev. **116**(18), 10513–10622 (2016).
4. P. Senellart, G. Solomon, and A. White, "High-performance semiconductor quantum-dot single-photon sources," Nat. Nanotechnol. **12**(11), 1026–1039 (2017).
5. P. Michler, A. Kiraz, C. Becher, W. V. Schoenfeld, P. M. Petroff, L. Zhang, E. Hu, and A. Imamoglu, "A quantum dot single-photon turnstile device," Science **290**(5500), 2282–2285 (2000).
6. Q. G. Chen, T. Y. Zhou, C. Y. He, Y. Q. Jiang, and X. Chen, "An in situ applicable colorimetric Cu^{2+} sensor using quantum dot quenching," Anal. Methods **3**(7), 1471–1474 (2011).
7. Y. Fan, H. Liu, R. Han, L. Huang, H. Shi, Y. Sha, and Y. Jiang, "Extremely high brightness from polymer-encapsulated quantum dots for two-photon cellular and deep-tissue imaging," Sci. Rep. **5**(1), 9908 (2015).
8. K. Welsher and H. Yang, "Multi-resolution 3D visualization of the early stages of cellular uptake of peptide-coated nanoparticles," Nat. Nanotechnol. **9**(3), 198–203 (2014).
9. Z. Pan, K. Zhao, J. Wang, H. Zhang, Y. Feng, and X. Zhong, "Near infrared absorption of $CdSe_xTe_{1-x}$ alloyed quantum dot sensitized solar cells with more than 6% efficiency and high stability," ACS Nano **7**(6), 5215–5222 (2013).
10. P. Zhao, Q. Xu, J. Tao, Z. Jin, Y. Pan, C. Yu, and Z. Yu, "Near infrared quantum dots in biomedical applications: current status and future perspective," Nanomed. Nanobiotechnol. **10**(3), 1483 (2017).

#323315 https://doi.org/10.1364/OE.26.011889
Journal © 2018 Received 14 Feb 2018; revised 6 Apr 2018; accepted 18 Apr 2018; published 24 Apr 2018

Optics EXPRESS

11. W. C. Law, Z. Xu, K. T. Yong, X. Liu, M. T. Swihart, M. Seshadri, and P. N. Prasad, "Manganese-doped near-infrared emitting nanocrystals for in vivo biomedical imaging," Opt. Express **24**(16), 17553–17561 (2016).
12. S. Rühle, "Tabulated values of the Shockley-Queisser limit for single junction solar cells," Sol. Energy **130**, 139–147 (2016).
13. B. Li, G. Zhang, Z. Wang, Z. Li, R. Chen, C. Qin, Y. Gao, L. Xiao, and S. Jia, "Suppressing the fluorescence blinking of single quantum dots encased in N-type semiconductor nanoparticles," Sci. Rep. **6**(1), 32662 (2016).
14. H. Qin, R. Meng, N. Wang, and X. Peng, "Photoluminescence intermittency and photo-bleaching of single colloidal quantum dot," Adv. Mater. **29**(14), 1606923 (2017).
15. M. Kuno, D. P. Fromm, H. F. Hamann, A. Gallagher, and D. J. Nesbitt, ""On"/"off" fluorescence intermittency of single semiconductor quantum dots," J. Chem. Phys. **115**(2), 1028–1040 (2001).
16. H. Yuan, E. Debroye, G. Caliandro, K. P. Janssen, J. van Loon, C. E. Kirschhock, J. A. Martens, J. Hofkens, and M. B. Roeffaers, "Photoluminescence blinking of single-crystal methylammonium lead Iodide perovskite nanorods induced by surface traps," ACS Omega **1**(1), 148–159 (2016).
17. S. Yamashita, M. Hamada, S. Nakanishi, H. Saito, Y. Nosaka, S. Wakida, and V. Biju, "Auger ionization beats photo-oxidation of semiconductor quantum dots: extended stability of single-molecule photoluminescence," Angew. Chem. Int. Ed. **54**, 3892–3896 (2015).
18. I. Potapova, R. Mruk, S. Prehl, R. Zentel, T. Basché, and A. Mews, "Semiconductor nanocrystals with multifunctional polymer ligands," J. Am. Chem. Soc. **125**(2), 320–321 (2003).
19. H. Cao, J. Ma, L. Huang, H. Qin, R. Meng, Y. Li, and X. Peng, "Design and synthesis of antiblinking and antibleaching quantum dots in multiple colors via wave function confinement," J. Am. Chem. Soc. **138**(48), 15727–15735 (2016).
20. Y. A. Wang, J. J. Li, H. Chen, and X. Peng, "Stabilization of inorganic nanocrystals by organic dendrons," J. Am. Chem. Soc. **124**(10), 2293–2298 (2002).
21. Z. J. Li, G. F. Zhang, B. Li, R. Y. Chen, C. B. Qin, Y. Gao, L. T. Xiao, and S. T. Jia, "Enhanced biexciton emission from single quantum dots encased in N-type semiconductor nanoparticles," Appl. Phys. Lett. **111**(15), 153106 (2017).
22. S. Hohng and T. Ha, "Near-complete suppression of quantum dot blinking in ambient conditions," J. Am. Chem. Soc. **126**(5), 1324–1325 (2004).
23. J. L. Nadeau, L. Carlini, D. Suffern, O. Ivanova, and S. E. Bradforth, "Effects of beta-mercaptoethanol on quantum dot emission evaluated from photoluminescence decays," J. Phys. Chem. C **116**(4), 2728–2739 (2012).
24. A. Biebricher, M. Sauer, and P. Tinnefeld, "Radiative and nonradiative rate fluctuations of single colloidal semiconductor nanocrystals," J. Phys. Chem. B **110**(11), 5174–5178 (2006).
25. V. Fomenko and D. J. Nesbitt, "Solution control of radiative and nonradiative lifetimes: A novel contribution to quantum dot blinking suppression," Nano Lett. **8**(1), 287–293 (2008).
26. V. Marx, "Probes: paths to photostability," Nat. Methods **12**(3), 187–190 (2015).
27. S. N. Sharma, Z. S. Pillai, and P. V. Kamat, "Photoinduced charge transfer between CdSe quantum dots and p-phenylenediamine," J. Phys. Chem. B **107**(37), 10088–10093 (2003).
28. S. Ravikumar, R. Surekha, and R. Thavarajah, "Mounting media: An overview," J. NTR. Univ. Health. Sci. **3**, 1–8 (2014).
29. A. Diaspro, F. Federici, and M. Robello, "Influence of refractive-index mismatch in high-resolution three-dimensional confocal microscopy," Appl. Opt. **41**(4), 685–690 (2002).
30. M. Hamada, S. Nakanishi, T. Itoh, M. Ishikawa, and V. Biju, "Blinking suppression in CdSe/ZnS single quantum dots by TiO2 nanoparticles," ACS Nano **4**(8), 4445–4454 (2010).
31. G. Zhang, L. Xiao, F. Zhang, X. Wang, and S. Jia, "Single molecules reorientation reveals the dynamics of polymer glasses surface," Phys. Chem. Chem. Phys. **12**(10), 2308–2312 (2010).
32. G. Zhang, L. Xiao, R. Chen, Y. Gao, X. Wang, and S. Jia, "Single-molecule interfacial electron transfer dynamics manipulated by an external electric current," Phys. Chem. Chem. Phys. **13**(30), 13815–13820 (2011).
33. H. W. Cheng, C. T. Yuan, J. S. Wang, T. N. Lin, J. L. Shen, Y. J. Hung, J. Tang, and F. G. Tseng, "Modification of photon emission statistics from single colloidal CdSe quantum dots by conductive materials," J. Phys. Chem. C **118**(31), 18126–18132 (2014).
34. B. Li, G. Zhang, C. Yang, Z. Li, R. Chen, C. Qin, Y. Gao, H. Huang, L. Xiao, and S. Jia, "Fast recognition of single quantum dots from high multi-exciton emission and clustering effects," Opt. Express **26**(4), 4674–4685 (2018).
35. Y. S. Park, W. K. Bae, J. M. Pietryga, and V. I. Klimov, "Auger recombination of biexcitons and negative and positive trions in individual quantum dots," ACS Nano **8**(7), 7288–7296 (2014).
36. S. Wang, C. Querner, T. Emmons, M. Drndic, and C. H. Crouch, "Fluorescence blinking statistics from CdSe core and core/shell nanorods," J. Phys. Chem. B **110**(46), 23221–23227 (2006).
37. J. Tang and R. A. Marcus, "Diffusion-controlled electron transfer processes and power-law statistics of fluorescence intermittency of nanoparticles," Phys. Rev. Lett. **95**(10), 107401 (2005).
38. M. Kuno, D. P. Fromm, H. F. Hamann, A. Gallagher, and D. J. Nesbitt, "Nonexponential "blinking" kinetics of single CdSe quantum dots: A universal power law behavior," J. Chem. Phys. **112**(7), 3117–3120 (2000).
39. F. Hu, B. Lv, C. Yin, C. Zhang, X. Wang, B. Lounis, and M. Xiao, "Carrier multiplication in a single semiconductor nanocrystal," Phys. Rev. Lett. **116**(10), 106404 (2016).

Optics EXPRESS

40. K. N. Lawrence, P. Dutta, M. Nagaraju, M. B. Teunis, B. B. Muhoberac, and R. Sardar, "Dual role of electron-accepting metal-carboxylate ligands: reversible expansion of exciton delocalization and passivation of nonradiative trap-states in molecule-like CdSe nanocrystals," J. Am. Chem. Soc. **138**(39), 12813–12825 (2016).
41. Y. Zhang, J. He, P. N. Wang, J. Y. Chen, Z. J. Lu, D. R. Lu, J. Guo, C. C. Wang, and W. L. Yang, "Time-dependent photoluminescence blue shift of the quantum dots in living cells: Effect of oxidation by singlet oxygen," J. Am. Chem. Soc. **128**(41), 13396–13401 (2006).
42. Y. W. Wang, Y. B. Zhang, and W. Q. Zhang, "First-principles study of the halide-passivation effects on the electronic structures of CdSe quantum dots," RSC Advances **4**(37), 19302–19309 (2014).
43. E. Arnspang Christensen, P. Kulatunga, and B. C. Lagerholm, "A single molecule investigation of the photostability of quantum dots," PLoS One **7**(8), e44355 (2012).
44. C. Galland, Y. Ghosh, A. Steinbrück, J. A. Hollingsworth, H. Htoon, and V. I. Klimov, "Lifetime blinking in nonblinking nanocrystal quantum dots," Nat. Commun. **3**(1), 908 (2012).
45. A. L. Efros, "Fine structure and polarization properties of band-edge excitons in semiconductor nanocrystals," Marcel Dekker, Inc: New York (2003).

1. Introduction

Colloidal quantum dots (QDs) have a wide range of applications such as photovoltaic cells [1], light emitting diodes [2, 3], single-photon sources [4, 5] and biomedical labelings [6–8] because of their wide absorption bands, narrow emission bands and high photoluminescence (PL) quantum yields. Among them, near-infrared (NIR) emitting QDs have attracted particular research interest for photovoltaic [9] and biomedical applications [10, 11]. On the one hand, the wider absorption bands of NIR QDs enable them to absorb photons ranging from ultraviolet to NIR wavelengths, and thus possess the desired band gaps for maximum power conversion in solar cells [12]. On the other hand, NIR QDs are especially advantageous for *in vivo* tissue imaging due to the low absorption coefficient and much reduced autofluorescence of tissue samples in the NIR range. However, the intrinsic photobleaching and PL intermittency of NIR QDs are roadblocks for most of their applications [13–16]. The PL intermittency (also called PL blinking) is attributed to the surface defect sites that trap photo-generated electrons or holes. Once the QD loses one of the photo-generated carriers, an ionized QD would be formed. When the ionized QD absorbs another photon, it would result in a three-carrier state called trion state. Either positive trion (two holes and one electron) state or negative trion (two electrons and one hole) state would initiate efficient Auger processes which act as low-radiative decay channels to quench the fluorescence of QD [14]. After the ionized QD is deionized, it recovers the neutral state and returns back to the bright state in the PL intensity trajectory. The photobleaching is speculated to be decomposition of QDs by photo-oxidation reactions [17]. The photobleaching and the PL intermittency can cause target-losing for single-particle tracking in biological systems, instable signals for single-photon sources as well as performance degradation for photovoltaics and optoelectronics. Hence, suppressing the undesired photobleaching and PL intermittency of core/shell QDs are extremely crucial for their applications.

Nowadays, many strategies have been utilized to suppress the photobleaching and the PL intermittency by passivating the surface defects and enhancing the structure stability of single QDs, including encapsulating single QDs with organic polymers [7, 18], uniform-alloy shells [19], alkyl ligands [20], and N-type semiconductor nanoparticles [13]. Nonetheless, some of these strategies require sophisticated synthesis processes or lead to changes in the PL properties of QDs. For example, when single QDs are encased in N-type semiconductor nanoparticles, the PL intensity would be reduced and the purity of single-photon emission would be degraded, despite the fact that fluorescence intermittency can be suppressed [21]. Alternatively, the photobleaching and PL intermittency have been shown to be partially inhibited by small reducing agents such as β-mercaptoethanol (BME), dithiothreitol, and mercaptoethylamine in mM concentrations [22–25]. These strategies, in which the single QDs are dissolved in a reducer solution, are post-processing and easy-to-use. *P*-Phenylenediamine (PPD), a commonly used reducing agent, has been widely applied to improve the photostability of dye molecules for microscopy and single-molecule spectroscopy [26]. Nevertheless, it has been reported that the low oxidation potential of PPD (0.26 V vs normal

Optics EXPRESS

hydrogen electrode) can act as an effective scavenger for photogenerated holes thus quenches the fluorescence of CdSe QDs without the shell structure [27]. Here, we use the PPD to effectively suppress the photobleaching and PL intermittency of single NIR CdSeTe/ZnS_{3ML} core/multi-shell QDs. PPD can reduce reactive oxygen species and suppress the photo-oxidation of QDs. Furthermore, it can passivate surface defect sites of single QDs and suppress photo-ionization. When single QDs are immersed in PPD solution, the survival time of single QDs, the on-state probability of PL intensity trajectories, and the total number of emitted photons are significantly increased, while the purity of single-photon emission is hardly changed. The suppression of the photobleaching and PL intermittency is beneficial to the applications of QDs in single-particle tracking, tissue imaging as well as single-photon sources.

2. Experimental section

2.1 Sample preparation

The NIR CdSeTe/ZnS_{3ML} core/multi-shell QDs (Qdot 800 Streptavidin Conjugate) were purchased from Thermo Fisher Scientific Inc. The QDs comprise a biotin-binding protein (streptavidin) covalently attached to QDs. Their maximum PL emission wavelength is ~800 nm. The PPD solution consists of 90% (volume) glycerin, 10% PBS, with PPD concentration in 5 mM and the pH is controlled within a range of 8.5-9.0. These chemicals were purchased from Sigma-Aldrich. The glycerin is commonly used as aqueous mounting medium in the biomedical sciences [28]. Phosphate buffered glycerin is commonly used to mount specimen for examination by microscopy and glycerol may be added to other agents to retard drying and cracking [29]. In order to study the PL properties of single QDs in the PPD, we fixed single QDs onto glass coverslip by a tethering protocol as follows [30]: 1) Glass coverslips were cleaned with sodium hypochlorite and hypochloric acid by dipping in the mixture solution and sonicating for 15 min. 2) The glass coverslips were repeatedly washed with milli-Q water and acetone. 3) The glass coverslips were silanized for 30 min at room temperature by dipping in a 0.5% solution of 3-aminopropyltriethoxysilane in acetone. 4) Repeating the step 2). 5) The glass coverslips were dipped in a 10 μM aqueous solution of biotin 3-sulfo N-hydroxysuccinimide ester for 30 min at room temperature. 6) The glass coverslips were thoroughly washed with milli-Q water. In the successive step, the QDs were tethered onto the biotinylated glass coverslips through biotin-streptavidin conjugate on the biotinylated coverslips for 30 min at room temperature. Unbound QDs were removed by being washed with milli-Q water. The PPD solution was dropped onto the glass coverslip tethered with single QDs and then placed a smaller glass coverslip onto PPD, and hot wax was applied to edges of glass coverslip to secure it. The single QDs without PPD was also spin-coated onto glass coverslip for a contrast experiment.

2.2 Experimental setup

Wide-field fluorescence imaging was employed for the fluorescence imaging of single QDs using an inverted microscope (Olympus IX71) equipped with an oil immersion objective (OLYMPUS, 100 × , 1.3NA) and an EMCCD camera (ProEM:512B, Princeton Instruments). A 635 nm diode laser (LDH-D-C-635, PicoQuant) worked in continuous wave (CW) mode was used as the excitation source. The excitation light was circularly polarized after passing through a λ/2 plate and a λ/4 plate and then went through a focus lens before entering the inverted microscope. PL photons were collected by the same objective and then passed through a dichroic mirror (Bright Line, Semrock) and a long pass filter (Bright Line, Semrock). The image was further magnified by 3.3 times with an additional lens (the resulting maximum view of the image is 24.6 × 24.6 μm^2) before reaching the EMCCD camera. Sequences of fluorescence images have been recorded with an exposure time of 100 ms.

Optics EXPRESS

Confocal scanning fluorescence microscope was employed to measure the PL intensity trajectories, lifetime and second-order correlation function of single QDs [31, 32]. The single QDs were excited using the same laser with an output pulse width of ~55 ps at a repetition rate of 5 MHz. The λ/2 plate and the λ/4 plate were used to change the linearly polarized laser into circular polarization light. The oil immersion objective was used to focus laser light onto the sample and collect fluorescence simultaneously. After passing through a dichroic mirror (Bright Line, Semrock), an emission filter (Bright Line, Semrock), and a notch filter (Bright Line, Semrock), the fluorescence was focused into a 100 μm pinhole for spatial filtering to remove out-of-focus photons. Finally, the PL was split by a 50/50 beam splitter cube into two beams and detected by two single-photon detectors (Excelitas, SPCM-AQRH-16-FC). A piezo-scan stage (Piezosystemjena, T-405-01) with an active x-y-z feedback loop mounted on the inversion microscope was used to scan the sample over the focused excitation spot. All signals including the synchronization of pulse laser and single photon detectors were fed into a time-tagged, time-resolved and time-correlated single photon counting (TTTR-TCSPC) data acquisition card (HydraHarp 400, PicoQuant), by which the time-dependence information for all of the detected photons can be recorded simultaneously [33, 34]. In this way, PL intensity trajectories, PL decay curves and second-order correlation function curves can be obtained simultaneously by post-processing photon streams. The spectra of QDs were measured by fluorescence spectrophotometer (F-7000, HITACHI).

3. Results and discussion

3.1 Suppressing photobleaching of single QDs with PPD

Photobleaching of single QDs on glass and in PPD was examined by continuous illumination and imaging under a fixed laser excitation power density of 2.7×10^6 mW/cm^2 for an hour. Here, when the QDs enter the dark state in their PL intensity trajectories for more than 200 s, we consider photobleaching of the single QDs to occur. PL images for single QDs on glass and in PPD before and after the one-hour measurements are shown in Fig. 1 (a-d), respectively. More than 80% of single QDs on glass photobleached after laser illumination for an hour, while the number of emitting single QDs in PPD is slightly reduced. For confocal scanning fluorescence microscopy, the laser in pulsed mode (7.4×10^{-11} J/pulse) was used to excite the single QDs for 600 s. The survival probability is 43% for single QDs on glass, while that is up to 99% for single QDs in PPD, as shown in Figs. 1(e) and 1(f). The distribution of survival times for single QDs on glass is also shown in Fig. 1(e). These results demonstrate that PPD can strongly suppress the photobleaching of single QDs, due to the fact that the PPD can reduce reactive oxygen species around QDs and passivation of surface defect sites [17]. We have also tested the photobleaching of single QDs in PPD under a larger laser power, as shown in Appendix A. The minimal PPD concentration for suppressing photobleaching has been tested, as shown in Appendix B.

Optics EXPRESS

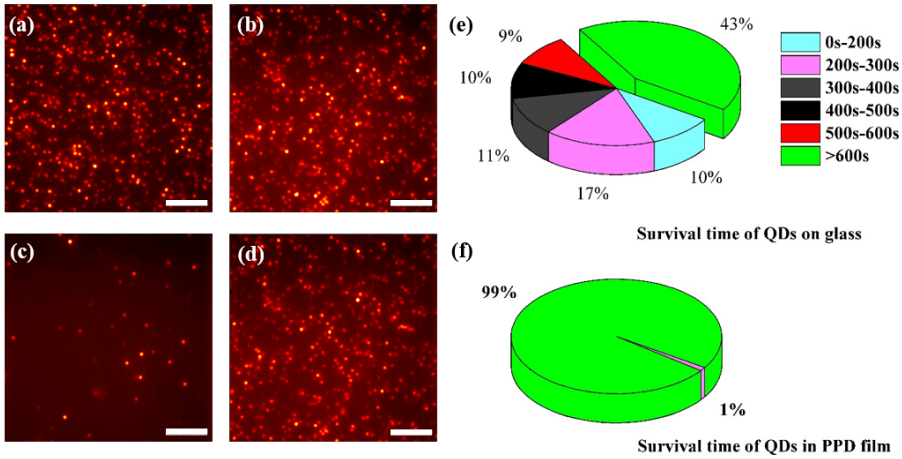

Fig. 1. Photoluminescence (PL) images for single QDs on glass (a) and in PPD (b) by using wide-field fluorescence imaging microscope before photo-excitation, respectively. PL images for the single QDs on glass (c) and in PPD (d) after the constant photo-excitation of an hour, respectively. (Scale bars: 5 μm.) (e, f) Pie charts of survival times for 100 studied single QDs on glass and in PPD by using confocal scanning fluorescence microscope, respectively.

3.2 Suppressing PL intermittency of single QDs with PPD

Figures 2(a) and 2(b) show two typical PL intensity trajectories and corresponding intensity histograms for single QDs on glass and in PPD, respectively. The trajectories were recorded with an integration time of 100 ms. PL intensity trajectories of single QDs on glass in Fig. 2(a) show obvious intermittencies and long-lasting dark states (also called off-state), and the corresponding intensity histogram mainly lies on the dark-state. In Fig. 2(b), for single QDs in PPD, the long dark states vanishes, and the corresponding intensity histogram mainly lies on the bright-state (also called on-state). Particularly, the durations at dark-state of QDs in PPD are very short, indicating the long dark state have been effectively suppressed. In general, these long dark states are due to positive trion states which are caused by the electron trap states (see the detailed analysis in Appendix C) [35]. Therefore, we conclude that the PPD can effectively remove the electron trap states.

In order to investigate the PL properties of single QDs in PPD, we have calculated the proportion of on-state for PL trajectories of 600 s for all measured single QDs. The threshold intensity, I_{th}, is defined to distinguish the on and off states, $I_{\text{th}} = I_{av} + 3\sigma$, where I_{av} is the average background and σ is its standard deviation [13]. Figure 2(c) shows the histograms of the proportion of on-state for single QDs on glass and in PPD. The proportion of on-state was obtained from the PL intensity trajectories for ~100 single QDs in both cases, and the histograms are fitted by Gaussian functions with the peak values of ~37% and ~85% for single QDs on glass and in PPD, respectively. These results show that the PPD significantly increases the proportion of on-state of single QDs. Moreover, the total number of emitted photons for single QDs in PPD and on glass is recorded by the TTTR-TCSPC data acquisition card for 10 min, as shown in Fig. 2(d). By fitting the histograms with Gaussian functions, the total number of emitted photons for single QDs in PPD is 2.3 times higher than that on glass.

Optics EXPRESS

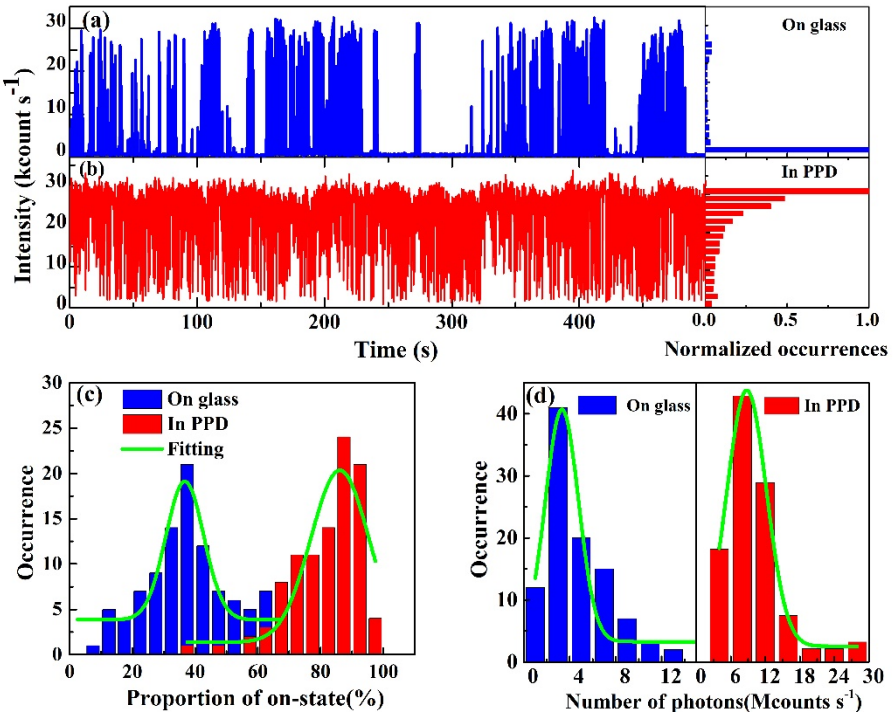

Fig. 2. (a) Typical PL trajectory and corresponding histogram for single QDs on glass. (b) Typical PL trajectories and corresponding histogram for single QDs in PPD. (c) Histograms of the proportion of on-state for ~100 studied single QDs on glass and in PPD, respectively. (d) Histograms of the number of emitted photons for ~100 studied single QDs on glass and in PPD, respectively.

3.3 Normalized probability densities of on- and off-state of single QDs

Here, we use normalized probability densities of on- and off-state to compare the PL intermittency of single QDs in the two cases. The on- and off-state probability densities $P_{on}(t)$ and $P_{off}(t)$ are defined as $P_i(t) = \frac{N_i(t)}{N_{i,total}(t)} \times \frac{1}{\Delta t_{i,av}}$ $(i = on\ or\ off)$, where $N_i(t)$ is the number of on- or off-state events of the duration time of t, $N_{i,total}(t)$ is the total number of on- or off-state events, and $\Delta t_{i,av}$ is average of the time intervals between the preceding and following events [15]. $P_{on}(t)$ and $P_{off}(t)$ of single QDs in both cases show a power law distribution at short time but deviate from this distribution at long time tails, as shown in Fig. 3. The truncated power law, $P_i(t) = A_i t^{-\alpha_i} \exp(-\mu_i t)$ $(i = on\ or\ off)$, Where A is the amplitude, α is the power law exponent, and μ is the saturation rate, can be used to fit these $P_{on}(t)$ and $P_{off}(t)$ [36–38]. Figure 3 shows that the typical normalized probability densities of on- and off-state for single QDs on glass and in PPD. More than 100 single QDs on glass and in PPD have been fitted to obtain the fitting parameters α and μ, respectively, as summarized in Table 1. We find that single QDs in PPD have a larger $1/\mu_{on}$ and a smaller $1/\mu_{off}$ than that of single QDs on glass, indicating the increased probabilities of on-state events and the decreased probabilities of off-state.

Optics EXPRESS

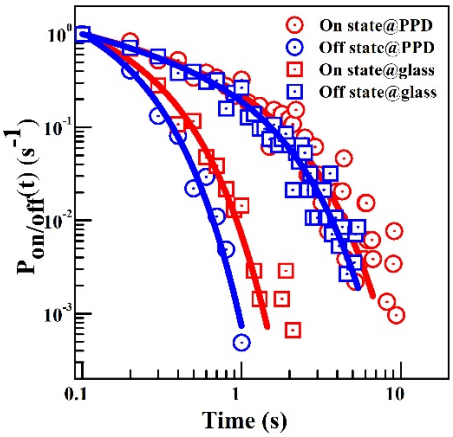

Fig. 3. Normalized probability densities of on-states ($P_{on}(t)$) and off-states ($P_{off}(t)$) for single QDs on glass and in PPD, respectively. The solid lines are well fitted by a truncated power law.

Table 1. Fitting parameters for normalized probability density of on-state ($P_{on}(t)$) and off-state ($P_{off}(t)$) for ~100 single QDs on glass and in PPD, respectively.

	α_{on}	$1/\mu_{on}$	α_{off}	$1/\mu_{off}$
QDs(on glass)	0.35 ± 0.22	0.59 ± 0.92	0.51 ± 0.32	1.21 ± 1.34
QDs(in PPD)	0.30 ± 0.17	1.67 ± 1.45	0.64 ± 0.46	0.20 ± 0.12

3.4 Fluorescence lifetimes, single photon purity and spectra of QDs in PPD

PL decay curves of single QDs on glass and in PPD are extracted from the on-state photons of PL trajectories by TTTR-TCSPC technique, as shown in Fig. 4(a). The dominant influence of the charged excitons on lifetimes can be distinguished [21, 39]. The blue and red lines represent the PL decays of single QDs on glass and in PPD, respectively. The PL decay curves can be fitted by a monoexponential function with the lifetime values of 131 ns (on glass) and 73.5 ns (in PPD), respectively. Figure 4(b) shows the histograms of the lifetimes for single QDs on glass and in PPD, respectively. The histograms of lifetimes were obtained from the ~120 single QDs in the two cases, which are fitted by Gaussian function with the average values of 132 ± 15 ns and 75 ± 12 ns for single QDs on glass and in PPD, respectively. This change of lifetimes is due to the different medium environments where single QDs were located in [25]. For single QDs in glycerin without PPD, the typical PL trajectory, PL decay curve, histogram of lifetimes, and testing of photobleaching have been shown in Appendix D. In addition, the typical second-order correlation function ($g^{(2)}(\tau)$) curve of single QDs in PPD is shown in Fig. 4(c). The peak of $g^{(2)}(\tau)$ at zero-time delay is rather low, which is same with that of single QDs on glass. Therefore, we conclude that the presence of PPD does not change the single-photon purity of single QDs. The emission spectrum of QDs in PPD has a redshift of 8 nm compared with that in glycerin without PPD, as shown in Fig. 4(d). The change of emission spectra indicates that the PPD can bond with the QDs surface to change the exciton confinement level, and thus change the spectra characteristics of QDs [40].

Optics EXPRESS

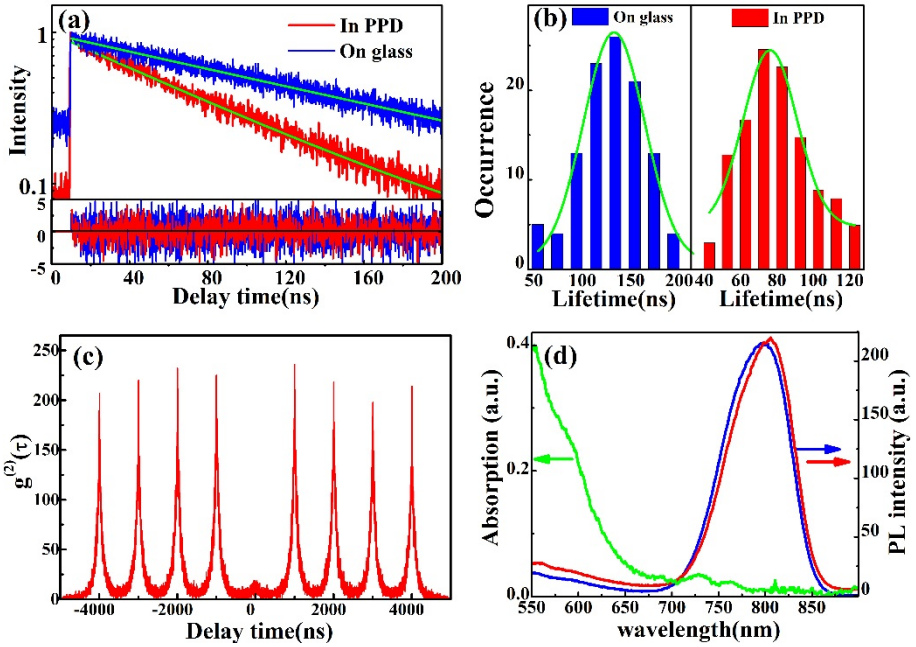

Fig. 4. (a) Fluorescence decay curves and monoexponential fits for single QDs on glass and in PPD. (b) Histograms of lifetimes for single QDs on glass (blue) and in PPD (red), respectively, with Gaussian fitting (green curves). (c) Typical second-order correlation function curve of single QDs in PPD with $g^{(2)}(0)$ of 0.064. (d) Absorption and emission spectra of CdSeTe/ZnS QDs, the green, blue and red lines represent the absorption spectrum, emission spectra of single QDs in glycerin without PPD and with PPD, respectively.

3.5 Discussion

Based on the abovementioned results, the mechanisms for suppressing photobleaching and PL intermittency are proposed in Fig. 5. PPD can be used as a high-efficient reducing agent to effectively remove reactive oxygen species (ROS) in solution. The ROS are generated from molecular oxygen by photoexcitation of the QDs [26], and alter the structure of QDs to cause the photobleaching [17, 41]. Therefore, the PPD can protect the QDs from photobleaching by effectively removing the ROS. In addition, the PPD can passivate surface defect sites of QDs to suppress the nonradiative recombination. The surface defect sites of CdSeTe/ZnS_{3ML} core/multi-shell QDs are mainly from the Zn atoms with the empty orbits. The N atoms of amine functional groups of PPD with redundant paired electrons can bond with Zn atoms in the form of coordination to passivate the surface defect sites to suppress the PL intermittency [42]. Some other antifade agents, such as BME, have also been suggested to bind to surface of QDs rather than to the polymer ligand to passivate the surface defect sites [22, 43]. We have also tested the effect of PPD on some other QDs with different ligands, such as CdSeTe/ZnS with TOPO/TOP, and CdSSe/ZnS with oleylamine. The PPD also can effectively suppress the photobleaching and the PL intermittency of these single QDs. Therefore, it also can be inferred that the PPD with relatively short chain length can pass through the ligand layer to QD surface to reduce surface defect sites [42]. Due to the QD surface bond with PPD, the exciton population [25] and confinement level can be changed [23], leading to reduced PL lifetimes (see the detailed analysis in Appendix E) and the redshift in emission spectra for the QDs in PPD. Also see Appendix F for the discussion on the quantum yields of QDs.

Optics EXPRESS

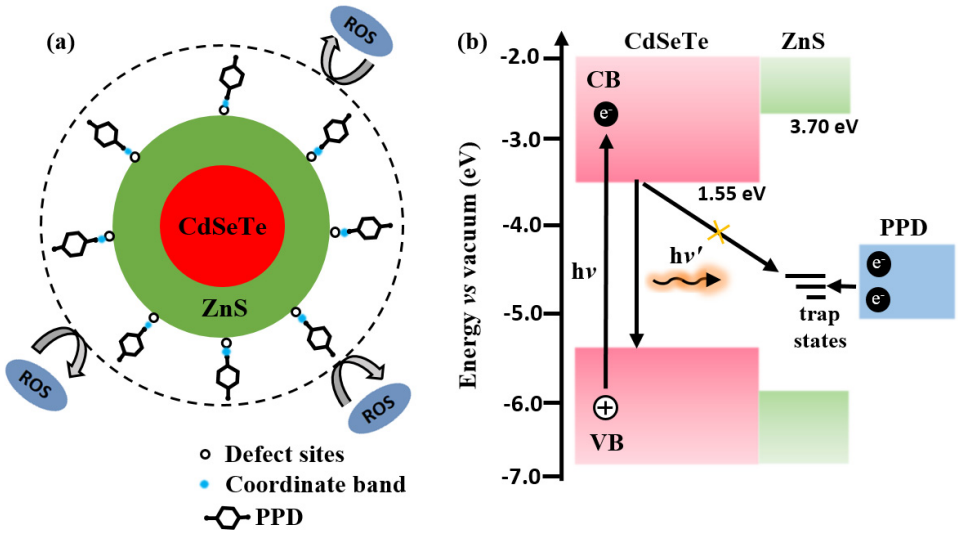

Fig. 5. (a) Possible interactions of PPD with single CdSeTe/ZnS_{3ML} core/multi-shell QDs. PPD can reduce reactive oxygen species (ROS) in solution and bind with surface defect sites to passivate the QDs to suppress PL intermittency. (b) Schematic of the excitation-relaxation cycle of single QD. The PPD removes electron trap states to suppress the photo-generated electron transfer from excited QD to trap states. CB and VB are the conduction band and valence band, respectively.

A schematic view of the excitation-relaxation cycle of single QD is shown in Fig. 5(b). Under photo-excitation, the formed electron-hole pair within the core emits a photon by radiative recombination, or the photo-generated electron is trapped by the trap states formed by the surface defect sites. Once the QD loses the photo-generated electron, a positive trion state would be formed under photo-excitation, which initiates Auger processes as an efficient low-radiative decay channel. When single QDs are immersed in PPD solution, the formation of positive trion states will be suppressed, and therefore the Auger low-radiative decay channel will be blocked. The PPD mainly suppresses the formation of positive trion states of single QDs (see Appendix C for details). Here the ZnS multi-shell of QDs can block the delocalization of photo-generated holes from the core to the QD surface. Therefore, PPD removes the surface defect sites of QDs rather than quenching the photo-generated holes, protecting QDs from photobleaching and PL intermittency.

4. Conclusions

Our study has demonstrated PPD to effectively suppress photobleaching and PL intermittency of single NIR CdSeTe/ZnS_{3ML} core/shell QDs in aqueous solution by removing reactive oxygen species and the electron trap states. We have shown that the survival probability of single QDs is up to 99% for single QDs in PPD under the same excitation condition and the on-state probability is significantly increased to 85%. Particularly the PL intermittency with long dark-state durations can be greatly reduced due to suppressed positive trion states of single QDs by PPD. Furthermore, the changes of PL lifetimes and spectra indicates the changes of exciton population and confinement level due to the PPD bonding with the QDs. The improvements of photobleaching and PL intermittency by PPD are favorable for the single-particle tracking, the tissue imaging *in vivo* and single-photon sources.

Appendix A: Testing the photobleaching of single QDs in PPD under a larger laser power

In order to check the photobleaching of single QDs in PPD, the 635 nm light from a diode-pumped solid-state laser (MLL-III-635, 500 mW, Changchun) was used as the excitation

Optics EXPRESS

source. This is the maximum power laser we have in the lab. ~40% of the laser power was lost after passing through various optical elements, and the final laser of ~300 mW was sent into the inverted fluorescence microscope from its back side. The wide-field fluorescence images for single QDs in PPD before and after the one-hour measurements under the excitation power density of 2.7×10^6 and 2.8×10^7 mW/cm^2 are shown in Fig. 6(a, c) and Fig. 6(b, d), respectively. The excitation power density of 2.8×10^7 mW/cm^2 corresponds to the maximum power of the laser. It seems that the change of the number of emitting single QDs under the maximum power is almost similar to that of 2.7×10^6 mW/cm^2 in main text.

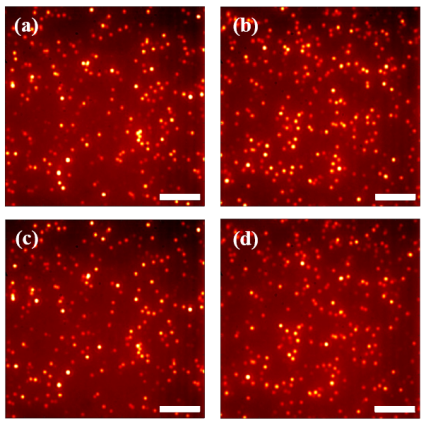

Fig. 6. PL images for single QDs in PPD by using wide-field fluorescence imaging microscope under the laser excitation power density of 2.7×10^6 mW/cm^2 before photo-excitation (a), and after the constant photo-excitation of an hour (c). PL images for single QDs in PPD under the laser excitation power density of 2.8×10^7 mW/cm^2 before photo-excitation (b) and after the one-hour measurements (d). (Scale bars: 5 μm.)

Appendix B: Testing the minimal PPD concentration level for suppressing photobleaching

We have tested the minimal PPD concentration level under the laser excitation power density of 2.8×10^7 mW/cm^2. PL images for single QDs in different PPD concentrations before and after the one-hour measurements are shown in Fig. 7. The PPD concentrations of 50 μM, 5 μM, 0.5 μM and 0 μM (in pure glycerin) correspond to the Figs. 7(a, e), (b, f), (c, g), and (d, h), respectively. We can see that the single QDs with the PPD concentration of 5 μM are largely photobleached in Figs. 7(b, f), while the number of emitting single QDs with the PPD concentration of 50 μM is slightly reduced in Figs. 7(a, e). Therefore, we suggest that ~50 μM may be close to the minimal PPD concentration to suppress photobleaching.

Optics EXPRESS

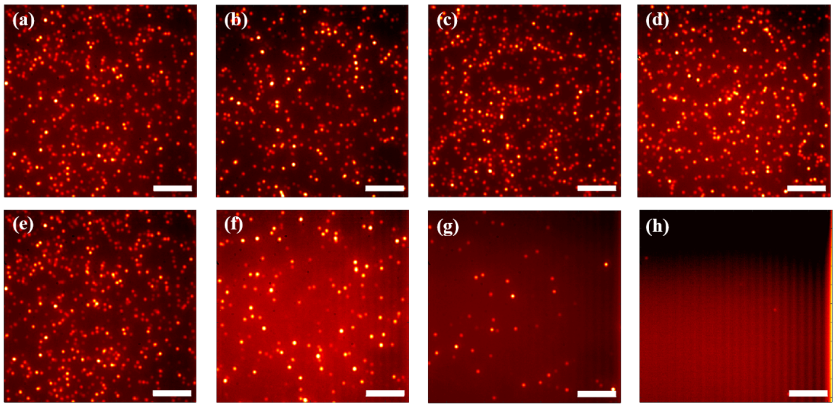

Fig. 7. PL wide-field fluorescence images for single QDs in different PPD concentrations before and after the one-hour measurements under the laser excitation power density of 2.8 × 10^7 mW/cm^2. The PPD concentrations are 50 μM (a, e), 5 μM (b, f), 0.5 μM (c, g) and 0 μM (d, h), respectively. (Scale bars: 5 μm.)

Appendix C: The PPD suppressing the formation of positive trion states of single QDs

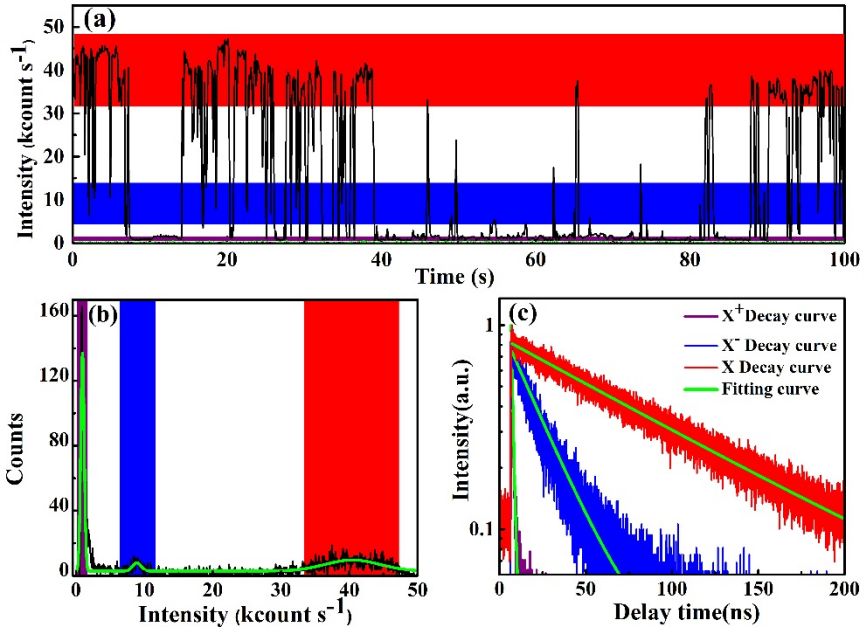

Fig. 8. (a) A typical PL trajectory with three different emissivities labeled by three color bands. The red, blue, and purple correspond to neutral exciton (X) states, negative trion (X-) state and positive trion (X +) states, respectively. (b) The corresponding histograms of PL intensities with three intensity peaks indicating by the same color bands. (c) The corresponding fluorescence decay curves and monoexponential fits for the three states. The lifetime values: τ (X) = 96 ns, τ (X-) = 21 ns and τ (X +) = 1.1 ns.

Figure 8 shows a typical PL intensity trajectory, a corresponding histogram of the PL intensity, and PL decay curves for single QDs on glass. The PL intensity trajectory with three different emissivities is labeled by three different color bands, as shown in Fig. 8(a), and the corresponding histogram of the PL intensity with three different intensity peaks are shown in Fig. 8(b). The three intensity peaks correspond to neutral exciton (X, red) states, negative

Optics EXPRESS

trion (X^-, blue) states and positive trion (X^+, purple) states, respectively [35]. In Fig. 8(c), the corresponding PL decay curves for the three states are obtained by recording arrival times of PL photons from the three different intensity bands of the PL trajectories by the TTTR-TCSPC technique. The three PL decay curves can be fitted by monoexponential functions to obtain three lifetime values of 96 ns (X states), 21 ns (X^- states) and 1.1 ns (X^+ states). The X^+ states are less efficient in emission and possess a shorter lifetime than the X^- states. This is because that the wavefunction of the photo-generated hole is significantly more localized than that of the photo-generated electron. The efficiency of non-radiative Auger recombination for a trion state depends on the wavefunction overlapping between carriers. The more localized of the wavefunction of a free charge is, the more efficient the Auger non-radiative recombination would be, and the less efficient and the shorter lifetime of the PL would be [14, 44]. By comparing the PL intensity trajectories without and with PPD in Fig. 2(a) and 2(b), it is found in Fig. 2(b) that the long dark states in the PL intensity trajectory caused by X^+ states are greatly reduced. Therefore, the PPD mainly suppresses the positive trion states of single QDs to reduce the PL intermittency.

Appendix D: Single QDs in glycerin without PPD

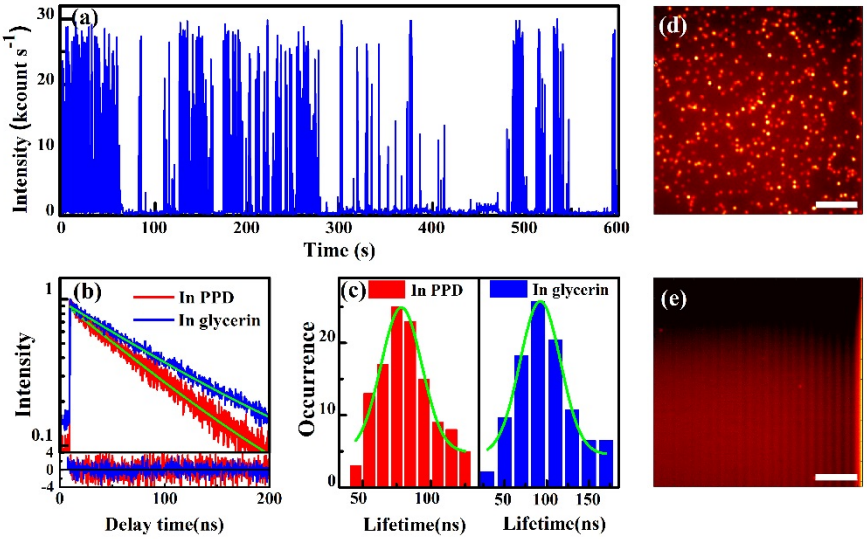

Fig. 9. (a) Typical PL trajectory for single QDs in glycerin. (b) Typical PL decay curves and monoexponential fits for single QDs in glycerin with PPD (red) and without PPD (blue). (c) Histograms of lifetimes for single QDs in glycerin with PPD (red) and without PPD (blue), respectively, with Gaussian fitting (green curves). (d, e) PL images for single QDs in glycerin by using wide-field fluorescence imaging microscope before photo-excitation and after the constant photo-excitation of an hour, respectively. (Scale bars: 5 μm.)

In order to test the effect of the glycerin on the fluorescence of single QDs, we have investigated the photobleaching and PL intermittency of single CdSeTe/ZnS_{3ML} core/shell QDs in glycerin without PPD. A typical PL intensity trajectory for single QDs in glycerin is shown in Fig. 9(a). We can observe from the figure that PL intensity trajectory of single QDs in glycerin shows obvious intermittencies and long-lasting dark states. PL decay curves of single QDs in glycerin are extracted from the on-state photons of PL trajectories by TTTR-TCSPC technique. A typical PL decay curve and the histogram of the lifetimes for single QDs in glycerin without PPD are shown in Fig. 9 (b, c). For comparison, the results for single QDs in glycerin with PPD are also shown in Fig. 9 (b, c). The PL decay curves can be fitted by a monoexponential function with the lifetime values of 95.2 ns (in glycerin) and 73.5 ns (in PPD), respectively. The histograms of lifetimes are fitted by Gaussian function with the

Optics EXPRESS

average values of 98 ± 15 ns and 75 ± 12 ns for single QDs in glycerin and in PPD, respectively. Therefore, the single QDs in PPD have smaller lifetime values than that in glycerin. And PL images for single QDs in glycerin under the excitation power density of 2.7 $\times 10^6$ mW/cm^2 before and after the one-hour measurements are shown in Fig. 9 (d, e). We can see that almost all single QDs photobleached after laser illumination for an hour.

Appendix E: The possible mechanism for the reduction of lifetime

The Ref [25]. has suggested a possible mechanism to explain the reduced PL lifetime. The PL lifetime of QDs is governed by the exciton population between the lower-energy dark and the higher-energy bright exciton states [45]. The reduced lifetime is due to the increasing exciton population of the bright exciton state, which leads to the acceleration of exciton recombination. QD surface defects, trap states and/or ligands would be changed when the antifade agents bind to QD surface. The changes were able to invert this energy ordering of the dark and bright exciton energy levels, and thereby lead to increasing population of the bright exciton state.

Appendix F: The quantum yields of QDs

We have measured the quantum yields of the CdSeTe/ZnS QDs in glycerin with PPD and without PPD. It is found that the quantum yields (~60%) are almost same in the two cases. The non-normalized emission spectra of QDs in glycerin with PPD and without PPD are shown in Fig. 4(d), and the peak values of the emission spectra with little difference also indicates little or no change in quantum yield in the two cases. The results are also consistent with the Ref. 25. Because both the measurements of quantum yield and emission spectra were implemented under the weak excitation conditions, the photoinduced blinking would not occur to reduce the quantum yields.

For single QDs measurements, the observed count rates in the PL intensity trajectories are linearly proportional to the fluorescence quantum yield. Thus, observation of the same peak emission rate in the PL intensity trajectories with and without PPD as shown in Fig. 2(b) and Fig. 9(a) implies that blinking suppression is achieved with little or no change in peak quantum yield. The reduction of PL lifetime concomitant with suppression of blinking and yet without reduction in peak quantum yield indicates that the presence of PPD can increase the radiative rate as well as the nonradiative rate [25].

Funding

National Key R & D Program of China (No. 2017YFA0304203); National Natural Science Foundation of China (NSFC) (Nos. 61527824, 61675119, U1510133, 11434007, 11504216, 61605104); PCSIRT (No. IRT13076, 1331KSC); Fund Program for the Scientific Activities of Selected Returned Overseas Professionals in Shanxi Province.